

The robustness of reverse-time migration for imaging noisy sparse foothills data

Laurence R. Lines and P.F. Daley

ABSTRACT

Seismic data from the Canadian Foothills are often noisy and sparsely sampled with missing traces. We show that reverse-time depth migration (RTM) provides a robust means of imaging sparse noisy data. Traditional RTM computes finite-difference (FD) solutions to the wave equation while back propagating the reflected wavefield to the reflector location at depth. The FD stencil will provide an effective means of interpolating missing traces during the migration process since this implicit interpolation essentially allows the seismic wavefield to heal itself during propagation. The FD operator also provides an effective means of suppressing random noise. Following earlier work by Zhu and Lines (1996), we illustrate the effectiveness of RTM on model data and real data from the Canadian Foothills.

INTRODUCTION

In the Canadian Foothills, seismic data are often recorded in rugged terrain, resulting in missing sources and receivers in the survey. Due to these logistical difficulties in recording, there are gaps in the seismic recording. Fortunately, seismic migration is reasonably robust with respect to missing information. In particular, the reverse-time depth migration method handles missing traces extremely well, as was demonstrated by Zhu and Lines (1996). In this study, we will examine the robustness of reverse-time migration on both poststack and prestack depth migration of Foothills data. We will explain this robustness by examining the nature of finite-differencing operations. We examine the limitations of where the migrations may be inadequate and make suggestions for future tests.

MODEL TESTS FOR SEISMIC RECORDS WITH MISSING INFORMATION

In order to test the effects of missing traces on seismic images, we use finite-difference synthetic seismograms for a realistic foothills model proposed by Kirtland-Grech et al. (1998). Figure 1 shows an exploding reflector synthetic seismogram for this model using a finite-difference grid of $25m$, containing 1330 seismic traces which emulate a stacked section. The reverse-time depth migration of this seismogram, as described in detail by Lines et al. (1999), is shown in Figure 2. The depth migration defines the subsurface layer boundaries, thrust fault locations and layer truncations quite clearly. We then performed tests in which we decimated traces from the seismic section and then examined the quality of the resulting reverse-time depth migrations. Figure 3 shows a record in which 4 groups of 40 traces for traces were decimated from Figure 1 including missing traces from 233-272; 360-399; 760-799; and 900-939. We then performed depth migrations on the section in Figure 3 to produce the migrated section in Figure 4.

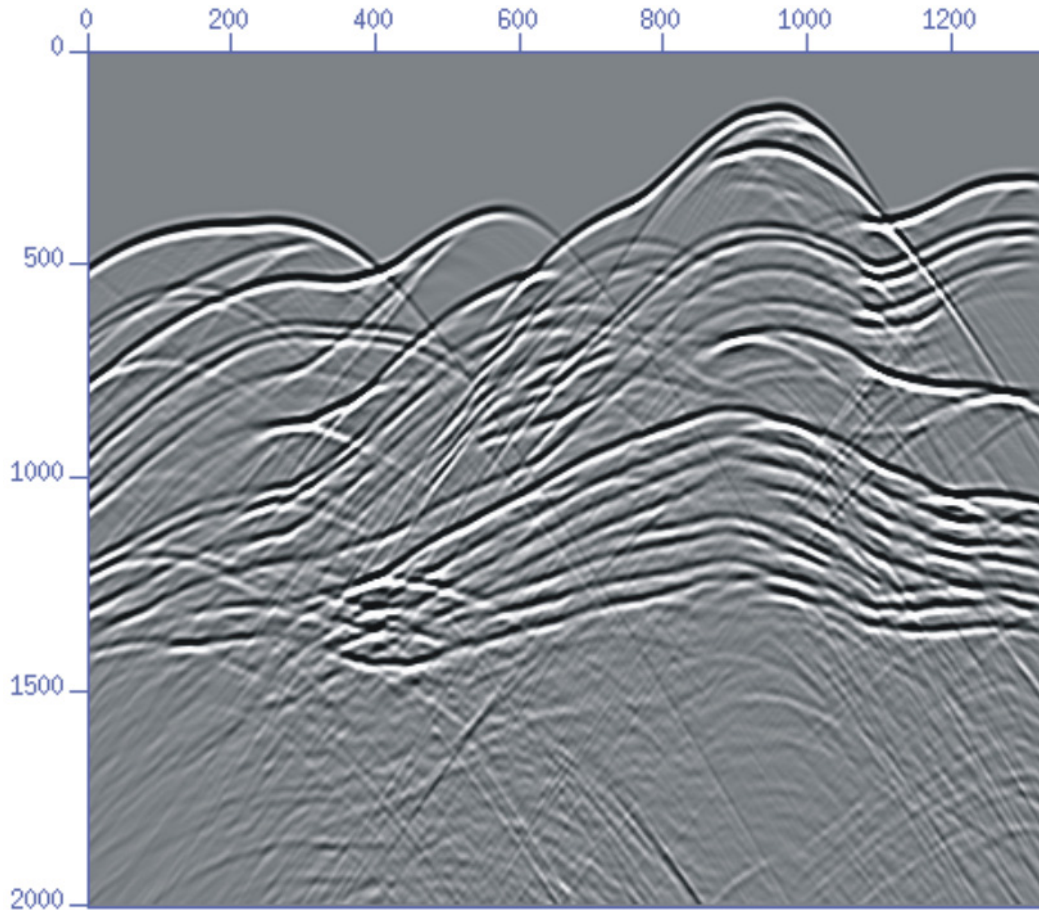


Fig. 1. The exploding reflector for the Grech-Spratt model represents an idealized stacked section. The section has 1350 traces with 2000 samples. Trace spacing is 25m and time sample interval is 2ms.

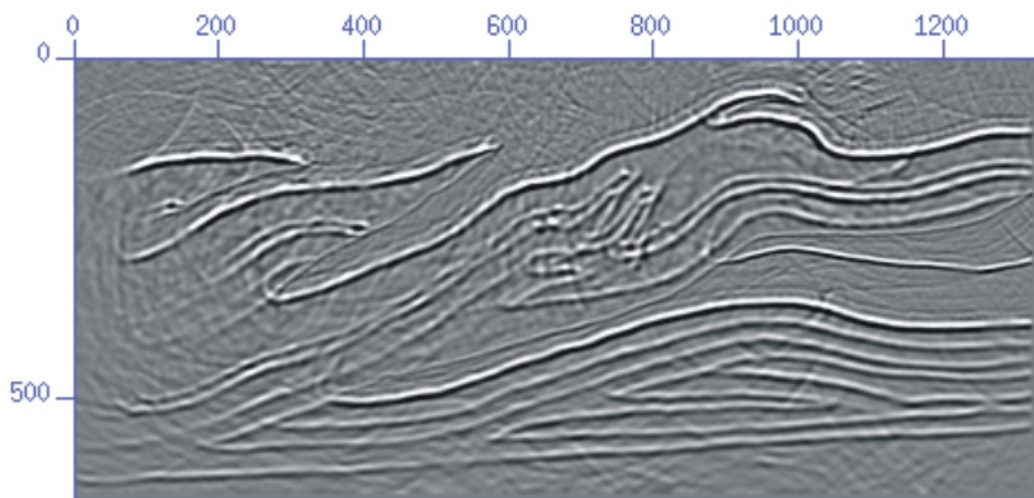


Fig. 2. Reverse-time depth migrated section of the stacked data in Figure 1. Spatial samples are separated by 25m intervals.

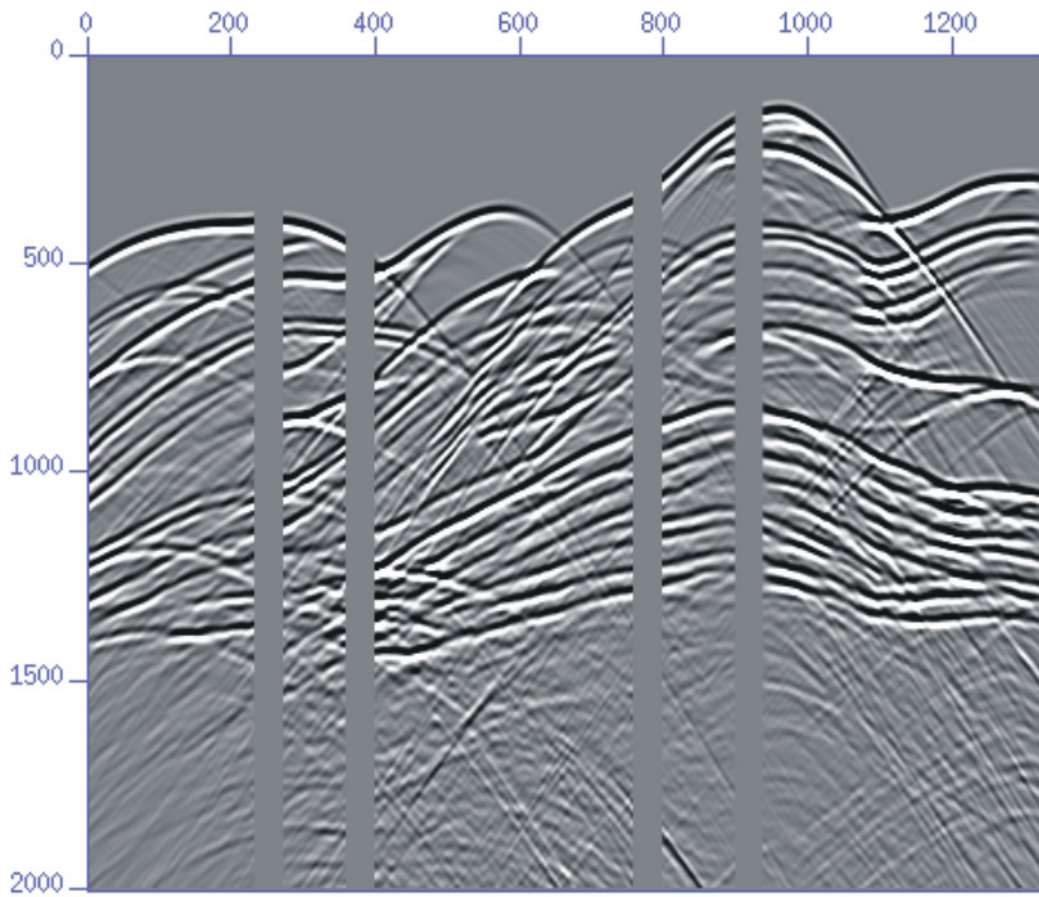


Fig. 3. Synthetic seismogram of model 1 with decimation for traces 233-272, 360-399, 760-799, and 930-999.

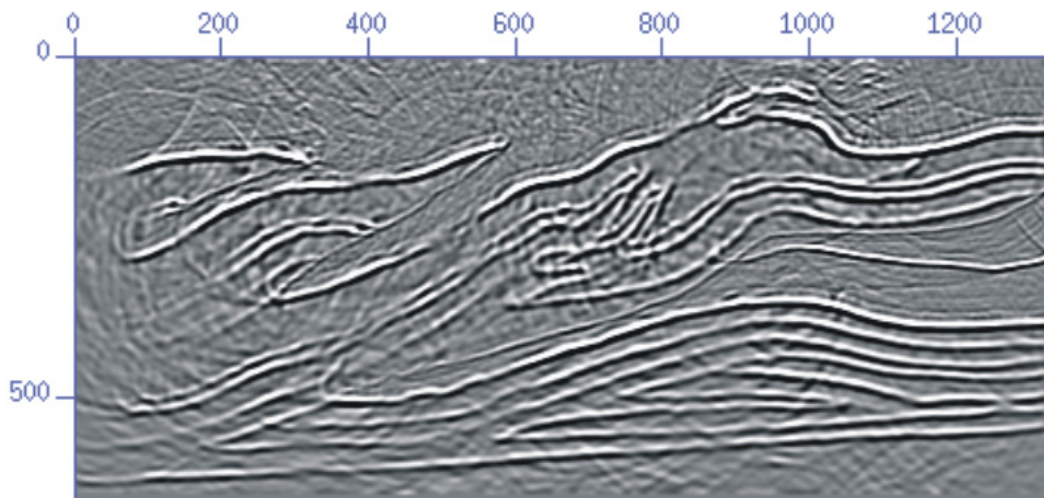


Fig. 4a. The reverse-time depth migrations of the data in Figure 3. We note blurring of reflections for footwall cutoffs beneath traces 233-272 and 360-399 and blurred anticlinal reflections between traces 900-939. Otherwise, the image is comparable to Figure 2.

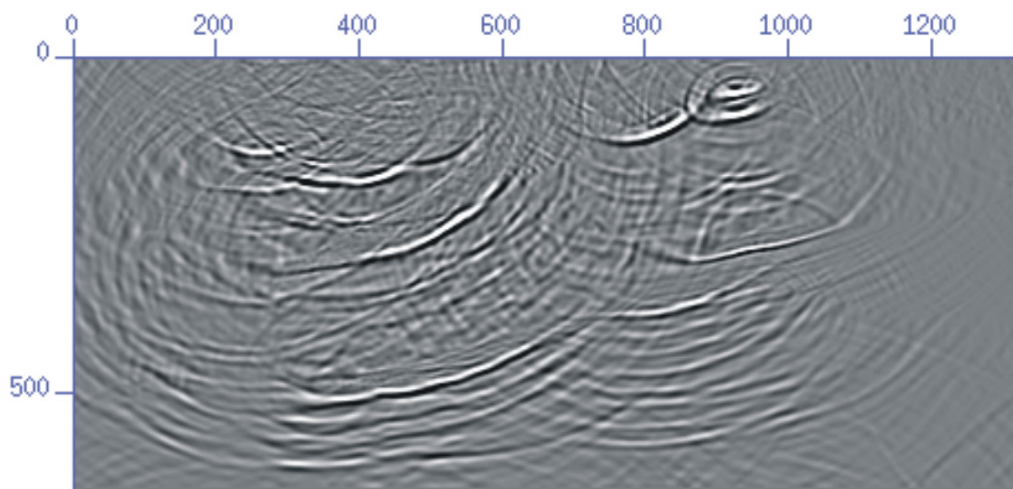


Fig. 4b. The difference between the optimum RTM of Figure 2 and the RTM of the section with missing data, as shown in Figure 4.

We note that while the linearly sloping reflections are hardly affected at all, there are some crucial parts of the subsurface in which it is difficult to define features in the migration of the decimated section (Figure 4a) as compared to the depth migration of the complete section (as shown in Figure 2). For example, we note that the footwall cutoffs are not clearly defined for the first group of missing traces (233-272) at depths of of 300-350 samples. The same is true for the second group of missing traces (360-399) at depth samples 480-520. There is also significant deterioration between anticlinal reflections for missing traces (900-939) at sample depths of about 100. Figure 4b shows a difference between the optimum migration of Figure 2 and the migration of the section with missing data, as shown in Figure 4a. Since the reflectors are dipping, we note that the imaging errors are not directly below the location of missing traces but are at the reflection points. Nevertheless, the interpretation of the RTM image of data with missing traces (Figure 4a) would probably be nearly identical to that of the ideal RTM (Figure 2).

From this poststack migration analysis, we can produce reliable depth migrations from records with missing traces as long as the missing traces are not in zones with cutoffs or truncated reflectors. Otherwise, reverse-time depth migration can handle data with significant gaps (40 traces in this case would correspond to missing data of 1000m), as long as the structures are simple. Of course, we generally do not know a priori where the complicated structures will exist on sections. Also, we note that the gaps are less than the Fresnel zones and this is a factor that we discuss later in this paper.

Having examined poststack depth migration, we now turn our attention to prestack depth migration and ask the following question. How many shots do we need to provide a reliable image of the subsurface? In this regard, it is worthwhile to examine an unpublished study by Lines and Zhu (1996) for the Marmousi model. In this study, the Marmousi data set was migrated using all the shot gathers, $\frac{1}{2}$ of the shot gathers, $\frac{1}{4}$ of the shot gathers, $\frac{1}{6}$ of the shot of

the shot gathers and 1/12 of the shot gathers. Figure 5 shows the results for the first three of these tests. It is interesting that image does not significantly deteriorate for decimated records – especially for deeper reflectors until we reach about ¼ of the shots being used. For prestack shot migration, the reverse-time migration method proves to be robust. To explain this behaviour for robust poststack and prestack reverse-time migration, we turn our attention to the application of finite-difference wave equation methods in reverse-time depth migration.

FINITE-DIFFERENCING IN REVERSE-TIME MIGRATION

In order to understand the robustness of reverse-time depth migrations on data with missing traces, it is useful to understand the nature of the finite-difference algorithm. The simplest form of the wave equation for a homogeneous medium is given by:

$$\nabla^2 u = \frac{1}{v^2} \frac{\partial^2 u}{\partial t^2} \quad (1)$$

For a grid spacing of h and a nodal point at, the second order approximation to the second derivative in x is

$$\frac{\partial^2 u}{\partial x^2} \approx \frac{1}{h^2} [u(x_0 + h) - 2u(x_0) + u(x_0 - h)] \quad (2)$$

If we substitute for this form of the second derivative approximation for derivatives in space and time, we note that in the computation at any point in time and space is related to its neighbours by a stencil of the form (1,-2,1). Otherwise stated, for each time step in wavefield computation, the wave is related to its neighbour. In essence, a wavefield is given by an averaging (interpolation) of surrounding nearest neighbours. If we went to higher orders, such as fourth order, there would be a wider given by (1/12, -16/12, 30/12, -16/12, 1/12).

Therefore in these finite-difference wave calculations in reverse-time migration, where we backward propagate traces in time, the traces with zero amplitude do not remain as zero values during propagation. In essence, the wavefield heals itself. Reverse-time migration has an implicit interpolation as shown by Zhu and Lines (1996).

The robustness of RTM on real data was shown by Wu et al. (1997) in the migration of the data set from Benjamin Creek, Alberta, which had several missing traces. Rather than interpolating trace values, the data were simply migrated and the influence of a few missing traces was not apparent.

At first glance, it may appear that reverse-time depth migration has obviated the problem of requiring interpolation for migration problems or the necessity of adequate sampling. If we examine the problems of spatial aliasing in regions of steep dip, we realize that this is simply not true. Aliased data will still pose a problem unless we can finely sample our data in space or apply smart interpolators to overcome the problem of aliased dipping events. For a discussion of the sampling problem in steeply dipping areas, we can examine the examples shown by Lines and Daley (2006).

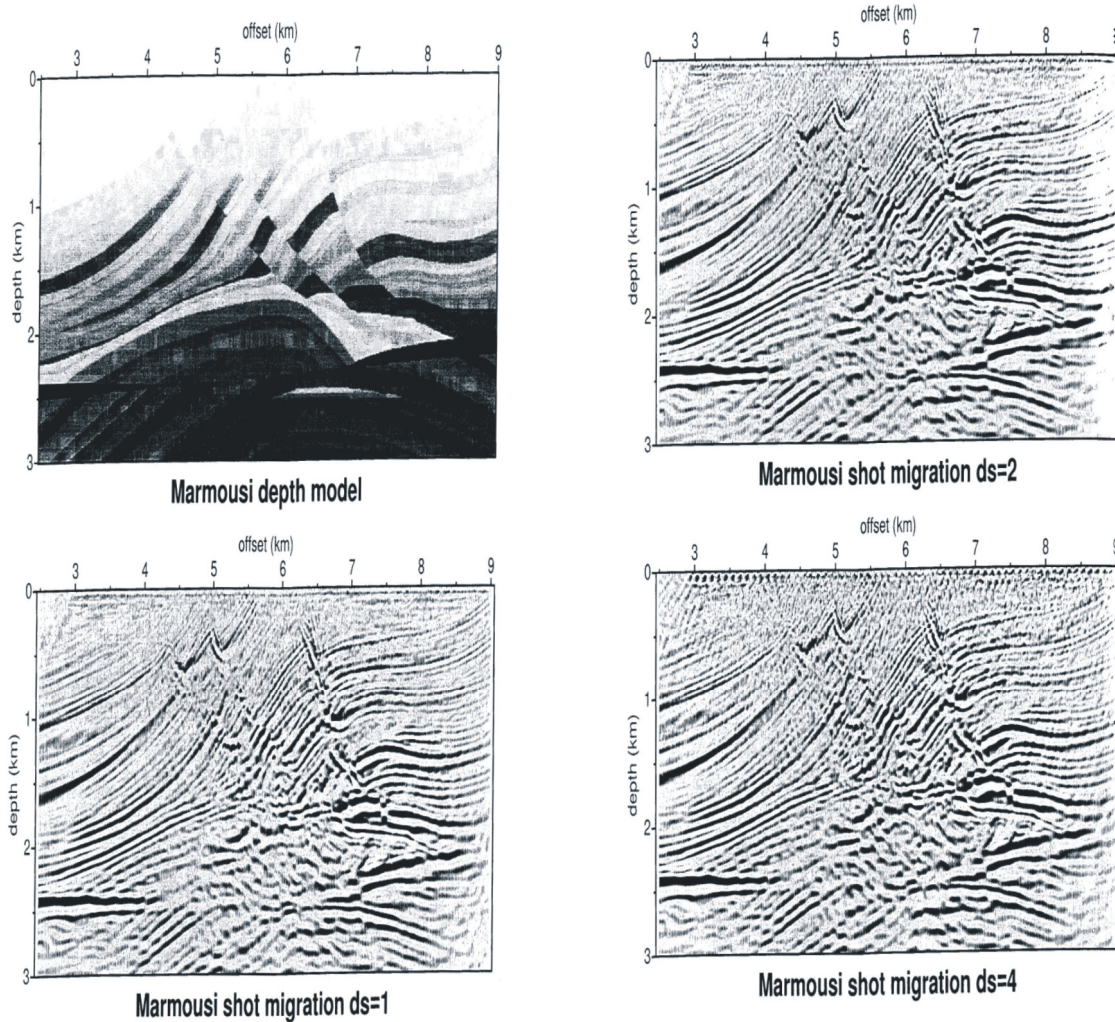


Fig. 5. Prestack reverse-time depth migrations of the Marmousi model using every shot (bottom left), every 2nd shot (top right) and every 4th shot (bottom right).

ROBUSTNESS OF IN REVERSE-TIME MIGRATION FOR IMAGING NOISY DATA

Now that we have shown that reverse-time migration is robust in its handling of seismic data with missing traces, we might also ask the question:

“How well can reverse-time migration handle data with additive random noise?”

In order to answer this question, we replace the zero traces of Figure 3 with noisy traces, as shown in Figure 6. In this figure, the missing traces are replaced by traces whose noise-to-signal ratio is 6.4. These traces were created by adding random numbers with zero mean and average absolute amplitude (AAA) of 6.4 to signal traces with an AAA of 1.0, in the same gap locations as in Figure 3.

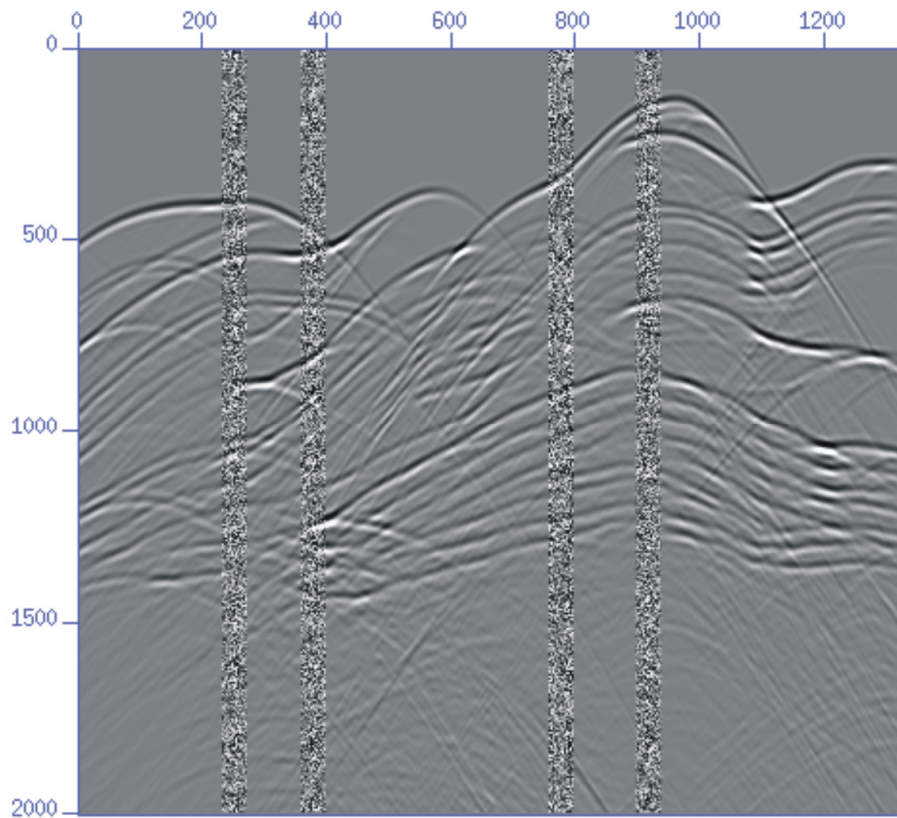


Fig. 6. Synthetic seismogram of model 1 with noise added to traces 233-272, 360-399, 760-799, and 930-999. Noise to signal ratio is 6.4 for these 160 traces.

The depth migration of the example in Figure 6 is shown in Figure 7. We note that while the depth migration, shown in Figure 8, appears slightly more noisy than the ideal migration in Figure 2, the RTM of noisy data may be even better than the RTM of missing traces. In summary, it is unlikely that our interpretation would be unduly damaged by migrating these noisy traces. This encouraging robustness is not surprising if we understand the effect of the FD stencil on random noise with zero mean.

The FD stencil is $(1/12, -16/12, 30/12, -16/12, 1/12)$ provides a running average of adjacent traces. Consider the effect of this operator on random noise with zero mean. A running average will provide a low pass filter on noise with zero mean. This filtering effect will greatly suppress the amplitudes of the random noise. Hence the migration of the noisy data will appear much like the migration of noiseless data.

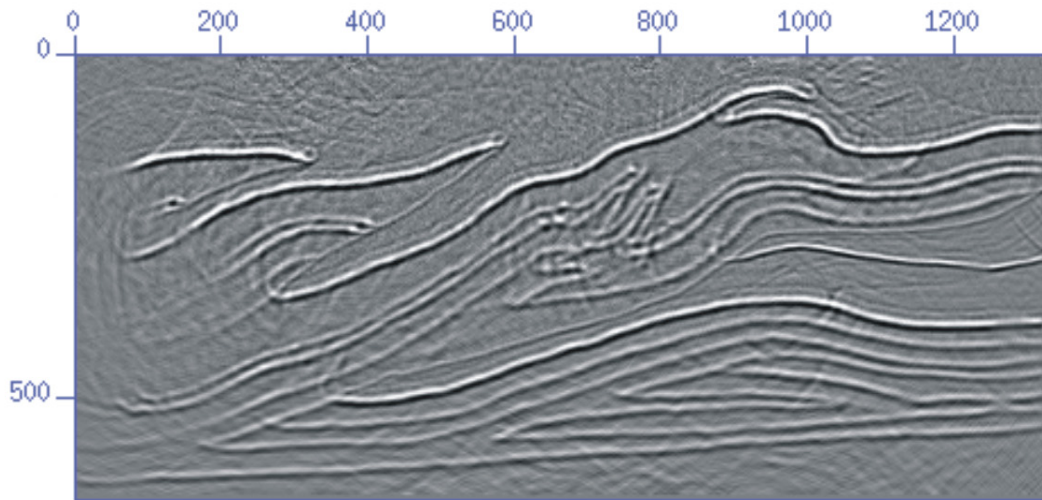


Fig. 7. The reverse-time depth migrations of the data in Figure 7.

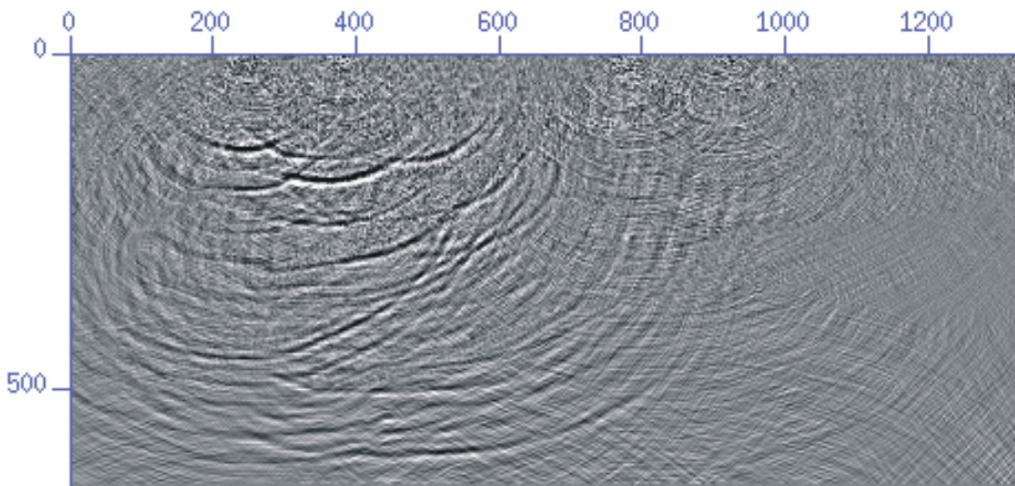


Fig. 8. The difference between the optimum RTM of Figure 2 and the RTM of the section with noisy traces, as shown in Figure 7.

At this point, we turn our attention to the migration of real data, from the Alberta foothills as originally shown by Lines and Daley (2006). As shown in Figure 9, the migration of the data with finer sampling (6.25m trace interval) shows better resolution for steeply dipping reflectors than the migration of data with coarser sampling (12.5 m trace interval). This is most apparent for the steeply dipping reflector in the box of Figure 9. For test of robustness, we migrate the finely sampled section with 30 traces deleted from 8125m to 8312.5m and compare the reflection quality. As shown in Figure 10, the reflection images are not appreciably different and it is unlikely that the structural interpretation would be significantly affected by the missing traces.

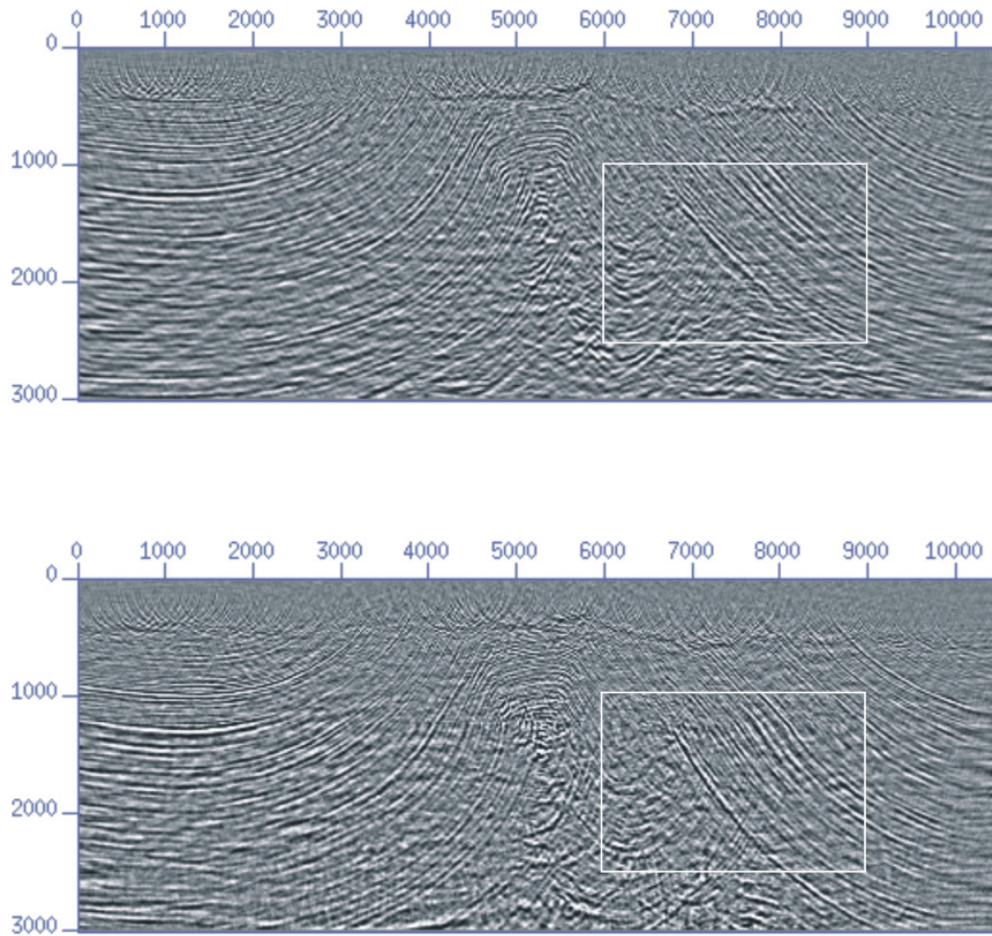


Fig. 9. Reverse-time migrations of the Shaw-Basing data with two different grid spacings. The upper section is migrated with grid spacing of $12.5m$ and the lower section is migration with $6.25m$. The slopes on the backthrust (in the box) are more clearly defined and less aliased in the lower section.

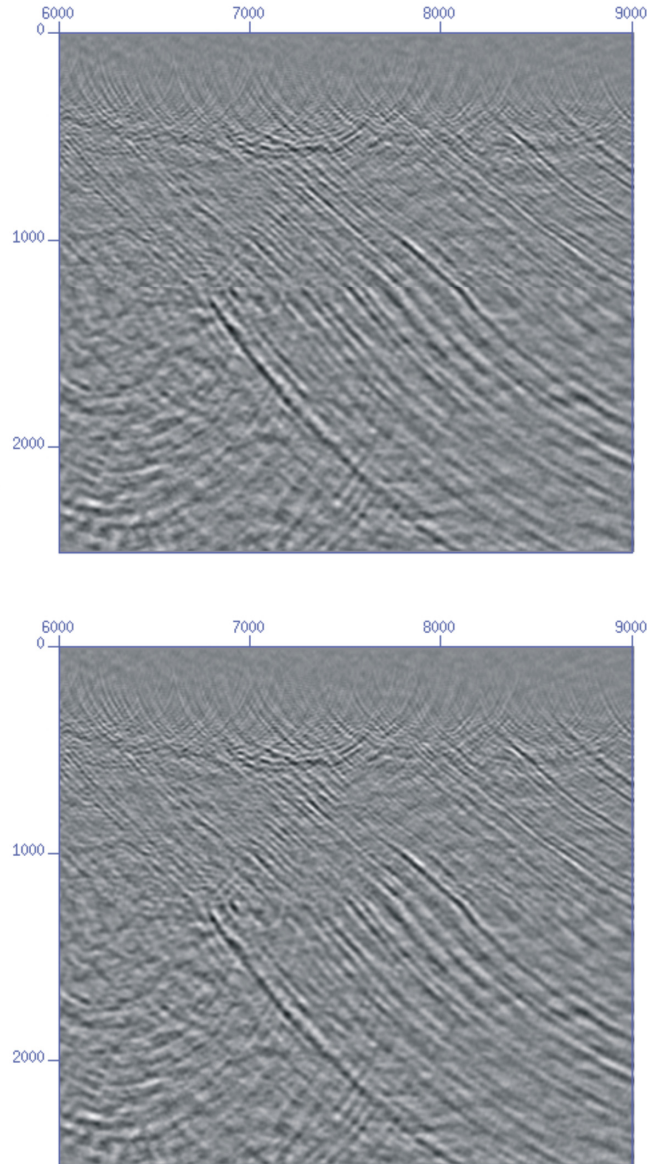


Fig. 10. Reverse-time migrations of the Shaw-Basing data for the highlighted zone. The top figure shows the migrated data for closely spaced samples in Figure 9. The bottom figure shows the migration of the same data with missing traces in the interval $8125m-8312.5m$.

FRESNEL ZONES AND RESOLUTION OF SPARSE DATA

In order to more completely understand the robustness of imaging sparse data and the degree of sparseness, we refer to “The Fresnel zone and its interpretive significance” by Lindsey (1989). In this paper, Lindsey demonstrates that the limits of spatial resolution are defined by the Fresnel diameter, F_D . For a seismic reflector at depth, Z , and seismic wavelength, λ , the Fresnel zone is given by $F_D = \sqrt{\lambda Z}$ and after migration is given by $F_D = \lambda/4$.

For many of our applications, the typical seismic wavelength was $100m$ and a typical depth was $1600m$. Hence, a Fresnel zone prior to migration would be $400m$, and our missing traces for Figure 9 spanned only $187.5m$. For such cases of reflectors at depth, the missing traces may be less than the limits of resolution. Additionally, the interpolation of the wavefield will be operating for longer distances and the wavefield “healing” has occurred.

CONCLUSIONS

Foothills data often have missing or noisy traces due to recording problems in difficult terrain. Fortunately, a few missing or noisy traces will not generally have a deleterious effect on reverse-time migrations except in areas of bed truncation (hanging wall and footwall cutoffs) or in areas of structural complexity. Both prestack and poststack reverse-time migrations are robust with respect to missing data. The reason for this robustness is seen by examining the nature of the finite-difference operations and the fact that there is an implicit interpolation in wave propagation calculations.

ACKNOWLEDGEMENTS

The author thanks Dr. Jinming Zhu, formerly of Memorial University of Newfoundland for providing computer codes for seismic modeling and migration in this study. Funding for this project was partly provided by an NSERC Discovery Grant.

REFERENCES

- Kirtland-Grech, G., Lawton, D.C., and Spratt, D., 1998, Numerical seismic modelling of complex fault fold structures in a mountainous setting: Foothills Research Project Annual Report, vol. 4, 1-1 – 1-35.
- Lindsey, J.P., 1989, The Fresnel zone and its interpretive significance: *The Leading Edge*, 10, 33-39.
- Lines, L.R., and Zhu, J., 1996, Prestack shot migration – How many shots are enough?: Memorial University Seismic Imaging Consortium Annual Report 1996, 13-17.
- Lines, L. R., Gray, S.H., and Lawton, D.C., 1999, Depth imaging of foothills seismic data: CSEG Publication, Calgary, Alberta.
- Lines, L.R., and Daley, P.F., 2006, Grid design in seismic modeling and migration, *Journal of Seismic Exploration*, 15, 1-14.
- Wu, W., Lines, L., Burton, A., Zhu, J., Jamison, W., and Bording, R.P., 1997, Prestack depth migration of an Alberta foothills data set – the Husky experience: *Geophysics*, 63, 392-398.
- Zhu, J., and Lines, L., 1996, Implicit interpolation in reverse-time migration, *Geophysics*, 62, 906-917.